# Femtosecond pulse erbium-doped fiber laser by a few-layer $MoS_2$ saturable absorber

**Hao Liu,[1] Ai-Ping Luo,[1] Fu-Zao Wang,[1] Rui Tang,[1] Meng Liu,[1] Zhi-Chao Luo,[1,*] Wen-Cheng Xu,[1,3] Chu-Jun Zhao,[2] and Han Zhang[2]**

[1]*Laboratory of Nanophotonic Functional Materials and Devices, School of Information and Optoelectronic Science and Engineering, South China Normal University, Guangzhou, Guangdong 510006, China*

[2]*Key Laboratory of Optoelectronic Devices and Systems of Ministry of Education and Guangdong Province, Shenzhen University, Shenzhen 518060, China*

[3]*e-mail: xuwch@scnu.edu.cn*

**Corresponding author: zcluo@scnu.edu.cn*

Received June 25, 2014; revised July 3, 2014; accepted July 3, 2014; posted July 7, 2014 (Doc. ID 214805); published July 31, 2014

We report on the generation of a femtosecond pulse in a fiber ring laser by using a polyvinyl alcohol (PVA)-based molybdenum disulfide ($MoS_2$) saturable absorber (SA). With a saturable optical intensity of 34 MW/cm$^2$ and a modulation depth of ~4.3%, the PVA-based $MoS_2$ SA had been employed with an erbium-doped fiber ring laser as a mode locker. The mode-locking operation could be achieved at a low pump threshold of 22 mW. A ~710 fs pulse centered at 1569.5 nm wavelength with a repetition rate of 12.09 MHz had been achieved with proper cavity dispersion. With the variation of net cavity dispersion, output pulses with durations from 0.71 to 1.46 ps were obtained. The achievement of a femtosecond pulse at 1.55 μm waveband demonstrates the broadband saturable absorption of $MoS_2$, and also indicates that the filmy PVA-based $MoS_2$ SA is indeed a good candidate for an ultrafast saturable absorption device. 

*OCIS codes:* (160.4330) Nonlinear optical materials; (140.4050) Mode-locked lasers; (140.3510) Lasers, fiber; (250.5530) Pulse propagation and temporal solitons.

http://dx.doi.org/10.1364/OL.39.004591

Ultrashort pulses, as an effective optical source to meet the growing needs of precision and speed in the fields of optical communication, spectroscopy, biomedicine, and material processing, have aroused much attention both in industry and scientific research. In the past decades, it has been demonstrated that the passively mode-locked fiber laser is a simple and economical way to achieve the ultrashort pulse [1,2]. To date, both the artificial saturable absorber (SA) [3–6] and real SA [7–24] were proposed to achieve ultrashort pulses in fiber lasers. Among them, due to their intrinsic environmental stability and the abundant saturable absorption materials, real SAs were in widespread use in ultrashort pulse fiber lasers. Meanwhile, SAs have experienced rapid development in recent years, being fabricated from materials from semiconductors to nanomaterials. Particularly, the newly emerging two-dimensional (2D) nanomaterials, such as graphene [11–14] and topological insulator (TI) [15–24], attracted strong attention in the ultrafast laser community due to their distinguished advantages such as ultrafast recovery time, controllable modulation depth, and easy fabrication.

Recently, it was found that the molybdenum disulfide ($MoS_2$), similarly to graphene, could be exfoliated into thin sheets to reveal extraordinary properties [25–27]. Since the ultrafast saturable absorption of 2D $MoS_2$ nanosheet was demonstrated by the open-aperture *Z*-scan technique at the 800 nm waveband [25], this material was proposed as an SA device to obtain ultrashort pulses in fiber lasers. In fact, $MoS_2$ could appear in two distinct morphologies: 2H phase (semiconducting) and 1T phase (metallic), which could support the broadband saturable absorption [26,27]. Zhang *et al.* reported the broadband saturable absorption at 400, 800, and 1060 nm wavebands and achieved ~800 ps pulse in a $MoS_2$-based ytterbium-doped fiber laser [27]. Enlightened by the broadband saturable absorption property in few-layer $MoS_2$, it would be naturally interesting to find out whether it can be developed as new type of SA at any laser wavelength. However, saturable absorption of $MoS_2$ at the telecommunication waveband has not been experimentally demonstrated. Moreover, the aforementioned $MoS_2$-based mode-locked fiber laser delivered pulse trains with durations of hundreds of picoseconds, while the femtosecond pulse has not yet been achieved. In fact, both the net cavity dispersion and quality of SA could affect the pulse characteristics, such as duration and stability. Therefore, fabricating a high-performance $MoS_2$ SA would contribute to achieving femtosecond pulses in fiber lasers with dispersion management. Compared to optical deposition [19,27] and spraying on a quartz plate [15,16], the filmy polymer composites method [11,12,22] would be more favorable to fabricating SAs because of their superiority in flexibility, cost-effectiveness, and controllability. Hence, it is interesting to know whether a femtosecond pulse at the communication waveband could be achieved by inserting a filmy $MoS_2$ SA into a fiber laser.

In this Letter, we obtained the femtosecond pulse from an anomalous-dispersion erbium-doped fiber (EDF) ring laser by using a filmy $MoS_2$ SA composited by polyvinyl alcohol (PVA). The crystalline structure of the as-prepared $MoS_2$ layer was confirmed by scanning electron microscope (SEM) and Raman spectrum. In the experiment, the PVA-based $MoS_2$ SA could provide a nonsaturable loss of 24% and a modulation depth of 4.3%. By inserting the $MoS_2$ SA into an EDF laser, the laser directly generated ~710 fs pulses centered at 1569.5 nm with a repetition rate of 12.09 MHz. In consideration of the influence of cavity dispersion, output pulse widths from

 

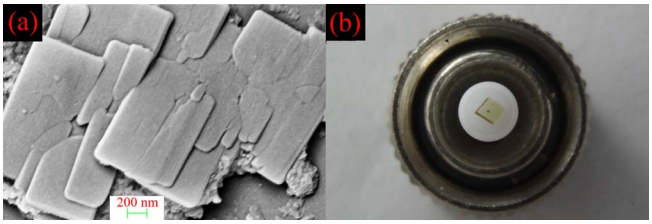


Fig. 1. (a) SEM image of $MoS_2$ nanosheets; (b) image of the fabricated fiber-compatible PVA-based $MoS_2$ SA.

0.71 to 1.46 ps were obtained with the variation of net cavity dispersion. The mode locking at the 1.55 μm waveband contributed to further demonstration of the broadband saturable absorption of the $MoS_2$ SA. Meanwhile, the achievement of femtosecond pulses confirmed that the $MoS_2$ could be indeed a good candidate for an ultrafast saturable absorption device.

With a layered structure like graphene and TI, the $MoS_2$ nanosheets could be synthesized by hydrothermal intercalation/exfoliation [26,27]. The detailed procedures for fabricating the $MoS_2$ nanosheets are the same as those reported in [27]. Figure 1(a) shows the SEM image of the as-prepared $MoS_2$ nanosheets, which exhibits the layered structure. After ultrasonicating for 1 h, the dispersion enriched $MoS_2$ isopropyl alcohol solution, with a concentration of ~0.018 mg/ml, is then mixed with an aqueous solution of PVA and ultrasonicated for 30 min. Evaporated at room temperature on a slide glass, the mixture is then formed into a filmy PVA-$MoS_2$ composite. Finally the prepared PVA-$MoS_2$ composite is transferred to the fiber facet between two fiber connectors for improving the compatibility with the fiber laser, as shown in Fig. 1(b).

To confirm that the $MoS_2$ nanosheets have been successfully embedded into the PVA with intact structure, we performed a Raman spectrum analysis on the samples. A Renishaw inVia micro-Raman system (Renishaw Inc., New Mills, UK) with an excitation wavelength of 514 nm was employed to manifest the atomic structural arrangement of $MoS_2$ and estimate the number of monolayers. The red curve in Fig. 2(a) represents the Raman spectrum of the filmy PVA-$MoS_2$ composite. Both the in-plane vibrational mode $E^1_{2g}$ at 383.2 $cm^{-1}$ and the out-of-plane vibrational mode $A^1_g$ at 407.4 $cm^{-1}$ were clearly exhibited, in agreement with previous studies of $MoS_2$ [28,29]. It should be noted that the existence of the $E^1_{2g}$ mode reveals the existence of 2H-$MoS_2$ [28]. In addition, it has been shown that the separation between the two modes decreases with decreasing thickness of the material, which is an effective way to estimate the number of layers in $MoS_2$ [28,29]. A frequency difference of ~24.2 $cm^{-1}$ was obtained in this work. Comparing to the previous works [28,29], it implies $MoS_2$ with thicknesses in the range of four to five monolayers. In order to rule out the influence of PVA, the Raman spectrum of the filmy pure PVA was also measured (blue curve). No evident Raman peaks exhibit in the range of 290–475 $cm^{-1}$. Therefore, one can conclude that the $MoS_2$ nanosheets embedded into the PVA matrix with their intact structures, indicating that the PVA could be an excellent host material for fabricating a convenient and reliable $MoS_2$ SA.

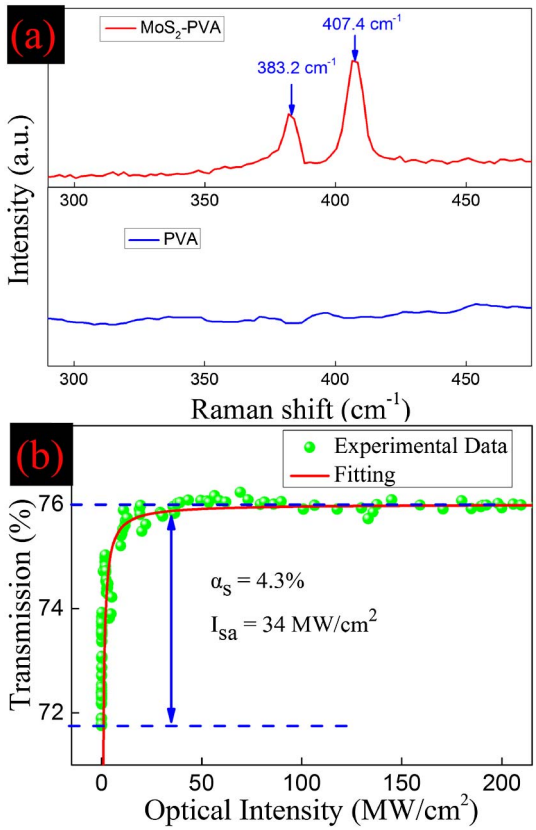


Fig. 2. (a) Raman spectra of $MoS_2$-PVA (red curve) and pure PVA (blue curve) and (b) measured nonlinear saturable absorption curve and corresponding fitting curve.

In order to better qualify the nonlinear optical characteristics of the fabricated filmy $MoS_2$ SA, the power-dependent transmission technique is employed to measure the nonlinear absorption. The experimental setup is the same as that in [17]. The pumping fiber laser used for saturable absorption measurement is an in-house-made femtosecond pulse source (center wavelength, 1554.4 nm; repetition rate, 26 MHz; pulse duration, ~500 fs). As presented in Fig. 2(b), the saturable absorption curve reveals a modulation depth of ~4.3%, and the nonsaturable loss is ~24%. Note that the weak nonsaturable loss may benefit from the good fiber compatibility and the few-layer $MoS_2$ flakes. In addition, it should be also noted that the saturable intensity of the fabricated PVA-based $MoS_2$ SA is 34 $MW/cm^2$, which is comparable to that of TI [19,22,23]. With such a low nonsaturable loss and saturable intensity, it would be predicted that the threshold of mode locking using the as-prepared $MoS_2$ SA can be significantly reduced. It means that the filmy PVA-$MoS_2$ composite could be a good candidate for an ultrafast SA with low insertion loss and low mode-locked threshold.

For further investigating the quality of the prepared $MoS_2$ SA, a fiber ring laser cavity based on the $MoS_2$ SA was proposed to achieve an ultrashort pulse. Figure 3 provides the schematic of the proposed fiber laser. A 4.8 m EDF with a group velocity dispersion parameter of ~ – 11.5ps/nm/km served as the gain medium. A wavelength division multiplexer (WDM) was utilized to inject the 976 nm pump light into the gain fiber. The

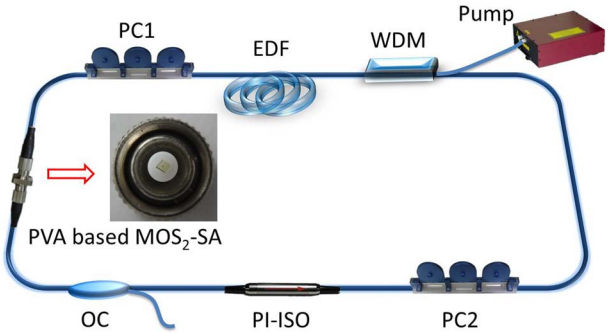


Fig. 3. Schematic of mode-locked fiber laser with a PVA-based $MoS_2$ SA.

adjustment of polarization state in the laser cavity was undertaken by a pair of polarization controllers (PCs). A polarization insensitive isolator was used to force the unidirectional operation of the laser cavity, and a 10/90 coupler was used to output the laser emission. The characteristics of the output light in both the frequency domain and time domain are monitored simultaneously by an optical spectrum analyzer (Anritsu MS9710C) and an oscilloscope (Agilent DSO-X 3052A) with a photodetector (New Focus P818-BB-35F, 12.5 GHz), respectively. A radio frequency spectrum analyzer (Advantest R3131A) was employed to record the RF spectrum of the mode-locking operation. In addition, the pulse duration was measured with a commercial autocorrelator (Femtochrome FR-103XL).

Benefiting from the low insertion loss of the filmy $MoS_2$ SA, continuous wave emission started at a pump power of about 10 mW and the self-started mode-locking occurred at about 22 mW. The stable femtosecond pulse operation at 46 mW was recorded in Fig. 4. Figure 4(a) shows the typical spectrum of mode-locking centered at 1569.5 nm with a 3 dB spectral bandwidth of 4.0 nm. The evident Kelly sidebands on the spectrum indicate that the mode-locked laser is operating in the soliton regime. Figure 4(b) presents the corresponding pulse train with

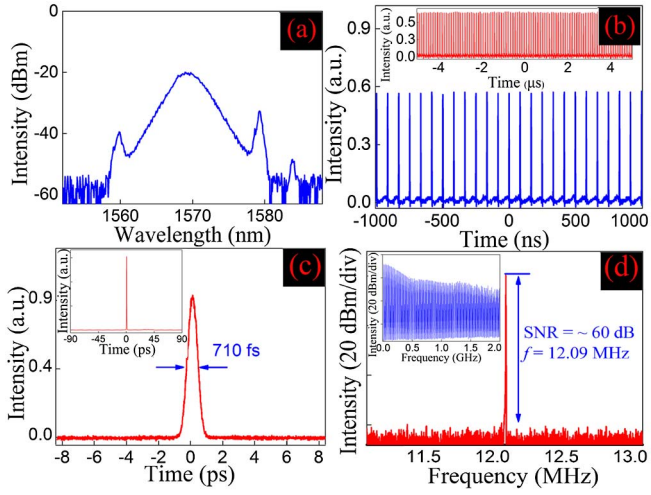


Fig. 4. Mode-locked operation. (a) Mode locked spectrum. (b) Corresponding pulse train; inset: pulse train with 10 μs span. (c) Corresponding autocorrelation trace; inset: autocorrelation trace with full range scan. (d) RF spectrum; inset: RF spectrum in 2 GHz span.

a repetition rate of 12.09 MHz, which was determined by the 17 m cavity length. In this case, the average output power is 1.78 mW, corresponding to an intracavity pulse power of 17.8 mW. Therefore, the pulse energy is 0.147 nJ. The uniform intensity distribution of the pulse train indicates the mode-locking operation was stable, as shown in the inset of Fig. 4(b). It should be noted that multipulse formation could be observed in the fiber laser when the pump power was high enough, for example ~150 mW. The autocorrelation trace in Fig. 4(c) shows that the fiber laser delivers a pulse train with a duration of 710 fs if the $Sech^2$ intensity profile was assumed. Thus, the time–bandwidth product is 0.346, indicating that the mode-locked pulse is slightly chirped. The full range scan of the autocorrelation trace is also shown in the inset. No pedestal shown on the autocorrelation trace reveals the excellent quality of mode locking. Moreover, the corresponding RF spectrum was measured with 300 Hz resolution bandwidth to further verify the stability of mode locking. As shown in Fig. 4(d), the fundamental peak is located at the fundamental repetition rate of 12.09 MHz with a signal-to-noise ratio of ~60 dB, manifesting the low-amplitude fluctuations and the high stability of pulse operation. The 2 GHz span RF spectrum in the inset is free of spectral modulation, suggesting that the fiber laser operates well in the cw mode-locking state. Note that the degradation stability of the SA was not observed for a long time (i.e., 24 h) when the pump power was kept at 46 mW. In the experiment, we have also checked the role of the $MoS_2$ SA in mode-locked operation by removing the $MoS_2$ SA from the fiber laser. In this case, even if the PCs were rotated and the pump power was adjusted in a large range, the passively mode-locked pulse could not be observed. The comparative results demonstrated that the saturable absorption of $MoS_2$ was responsible for the mode-locked operation of the proposed fiber laser. The damage threshold of the PVA-based $MoS_2$ SA was also tested by increasing the pump power. Typically, it was found that the damage threshold of the $MoS_2$ SA composited by PVA was about 240 mW pump power. Note that the peak intensity of the femtosecond pulse inside the SA is 1340 W when the stable femtosecond pulse was obtained with a pump power of 46 mW. Thus, it is far from the damage threshold of the PVA-based $MoS_2$ SA.

As we know, the pulse characteristics, such as duration and stability, could be affected by the intrinsic recovery time of the material, the fabrication method of the mode locker, and the cavity dispersion. In the experiment, the relationship between the pulse width and net cavity dispersion has also been investigated. We

**Table 1. Optical Parameters of $MoS_2$ Mode-Locked Fiber Laser**

| Cavity Length (m) | Net Dispersion ($ps^2$) | Frequency (MHz) | Pulse Width (ps) |
|---|---|---|---|
| 35.55 | −0.611 | 5.78 | 1.46 |
| 27.80 | −0.438 | 7.39 | 1.27 |
| 22.65 | −0.324 | 9.07 | 1.13 |
| 18.75 | −0.238 | 10.96 | 0.96 |
| 17.00 | −0.199 | 12.09 | 0.71 |

managed the net cavity dispersion by gradually varying the length of single-mode fiber while maintaining the 4.8 m EDF and SA. Table 1 includes five groups of experimental data, which show the relationship between cavity dispersion and laser performance. The pulse width and the net cavity dispersion vary from 0.71 to 1.46 ps and −0.199 to −0.611 $ps^2$, respectively, via controlling the length of single-mode fiber corresponding to the repetition rate of 12.09 to 5.78 MHz. Compared to graphene [11] and TI [22,23], $MoS_2$ could support comparable ultrashort pulses in the fiber laser with approximate net cavity dispersion. Note that the 710 fs pulse duration was achieved by using the fabricated $MoS_2$ SA. However, it is expected that a shorter pulse duration could be achieved by further engineering the cavity dispersion. The experimental results reveal that the $MoS_2$ could be a good candidate of ultrafast saturable absorption device.

In conclusion, we have fabricated a PVA-based $MoS_2$ SA, which shows a modulation depth of ∼4.3% and a saturable optical intensity of 34 $MW/cm^2$. Inserting the as-prepared $MoS_2$ SA into an EDF ring laser, the stable ∼710 fs pulse centered at 1569.5 nm with a fundamental repetition rate of 12.09 MHz was achieved. Moreover, the dependence of pulse width on the net cavity dispersion has been also investigated. The results provide the first demonstration of the saturable absorption of $MoS_2$ at the 1.55 μm waveband and also indicate that the filmy PVA-based $MoS_2$ SA indeed could be a simple, low-cost, low-insertion-loss, ultrafast saturable absorption device for applications such as mode-locked fiber lasers.

We would like to thank Yong-Fang Dong (South China Normal University) for help in measuring the Raman spectra. This work was supported in part by the National Natural Science Foundation of China (Grant Nos. 61378036, 61307058, 11304101) and the PhD Start-up Fund of Natural Science Foundation of Guangdong Province, China (Grant No. S2013040016320), and Z. C. Luo acknowledges the financial support from Zhujiang New-star Plan of Science & Technology in Guangzhou City (Grant No. 2014J2200008).

**References**

1. U. Keller, Nature **424**, 831 (2003).
2. M. E. Fermann and I. Hartl, Nat. Photonics **7**, 868 (2013).
3. M. J. Guy, D. U. Noske, and J. R. Taylor, Opt. Lett. **18**, 1447 (1993).
4. F. Ö. Ilday, J. R. Buckley, W. G. Clark, and F. W. Wise, Phys. Rev. Lett. **92**, 213902 (2004).
5. D. Y. Tang and L. M. Zhao, Opt. Lett. **32**, 41 (2007).
6. Z. C. Luo, Q. Y. Ning, H. L. Mo, H. Cui, J. Liu, L. J. Wu, A. P. Luo, and W. C. Xu, Opt. Express **21**, 10199 (2013).
7. O. Okhotnikov, A. Grudinin, and M. Pessa, New J. Phys. **6**, 177 (2004).
8. F. Wang, A. G. Rozhin, V. Scardaci, Z. Sun, F. Hennrich, I. H. White, W. I. Milne, and A. C. Ferrari, Nat. Nanotechnol. **3**, 738 (2008).
9. S. Yamashita, J. Lightwave Technol. **30**, 427 (2012).
10. X. M. Liu, D. D. Han, Z. P. Sun, C. Zeng, H. Lu, D. Mao, Y. D. Cui, and F. Q. Wang, Sci. Rep. **3**, 2718 (2013).
11. Q. L. Bao, H. Zhang, Y. Wang, Z. H. Ni, Y. L. Yan, Z. X. Shen, K. P. Loh, and D. Y. Tang, Adv. Funct. Mater. **19**, 3077 (2009).
12. H. Zhang, Q. L. Bao, D. Y. Tang, L. M. Zhao, and K. Loh, Appl. Phys. Lett. **95**, 141103 (2009).
13. Z. Sun, T. Hasan, F. Torrisi, D. Popa, G. Privitera, F. Wang, F. Bonaccorso, D. M. Basko, and A. C. Ferrari, ACS Nano **4**, 803 (2010).
14. Z. Q. Luo, M. Zhou, J. Weng, G. M. Huang, H. Y. Xu, C. C. Ye, and Z. P. Cai, Opt. Lett. **35**, 3709 (2010).
15. C. J. Zhao, H. Zhang, X. Qi, Y. Chen, Z. T. Wang, S. C. Wen, and D. Y. Tang, Appl. Phys. Lett. **101**, 211106 (2012).
16. C. J. Zhao, Y. H. Zou, Y. Chen, Z. T. Wang, S. B. Lu, H. Zhang, S. C. Wen, and D. Y. Tang, Opt. Express **20**, 27888 (2012).
17. Z. C. Luo, M. Liu, H. Liu, X. W. Zheng, A. P. Luo, C. J. Zhao, H. Zhang, S. C. Wen, and W. C. Xu, Opt. Lett. **38**, 5212 (2013).
18. M. Liu, N. Zhao, H. Liu, X. W. Zheng, A. P. Luo, Z. C. Luo, W. C. Xu, C. J. Zhao, H. Zhang, and S. C. Wen, IEEE Photon. Technol. Lett. **26**, 983 (2014).
19. Z. Q. Luo, Y. Z. Huang, J. Weng, H. H. Cheng, Z. Q. Lin, B. Xu, Z. P. Cai, and H. Y. Xu, Opt. Express **21**, 29516 (2013).
20. L. P. Sun, Z. Q. Lin, J. Peng, J. Weng, Y. Z. Huang, and Z. Q. Luo, Sci. Rep. **4**, 4794 (2013).
21. H. Yu, H. Zhang, T. Wang, C. J. Zhao, B. Wang, S. C. Wen, H. J. Zhang, and J. Wang, Laser Photon. Rev. **7**, L77 (2013).
22. H. Liu, X. W. Zheng, M. Liu, N. Zhao, A. P. Luo, Z. C. Luo, W. C. Xu, H. Zhang, C. J. Zhao, and S. C. Wen, Opt. Express **22**, 6868 (2014).
23. J. Sotor, G. Sobon, K. Grodecki, and K. M. Abramski, Opt. Express **22**, 13244 (2014).
24. J. Lee, J. Koo, Y. M. Jhon, and J. H. Lee, Opt. Express **22**, 6165 (2014).
25. K. Wang, J. Wang, J. Fan, M. Lotya, A. O'Neill, D. Fox, Y. Feng, X. Zhang, B. Jiang, Q. Zhao, H. Zhang, J. N. Coleman, L. Zhang, and W. J. Blau, ACS Nano **7**, 9260 (2013).
26. J. Zheng, H. Zhang, S. H. Dong, Y. P. Liu, C. T. Nai, H. S. Shin, H. Y. Jeong, B. Liu, and K. P. Loh, Nat. Commun. **5**, 2995 (2014).
27. H. Zhang, S. B. Lu, J. Zheng, J. Du, S. C. Wen, D. Y. Tang, and K. P. Loh, Opt. Express **22**, 7249 (2014).
28. C. Lee, H. Yan, L. E. Brus, T. F. Heinz, J. Hone, and S. Ryu, ACS Nano **4**, 2695 (2010).
29. H. Li, Q. Zhang, C. C. R. Yap, B. K. Tay, T. H. T. Edwin, A. Olivier, and D. Baillargeat, Adv. Funct. Mater. **22**, 1385 (2012).